Materials Science & Engineering B 231 (2018) 1–4

Contents lists available at ScienceDirect

Materials Science & Engineering B

journal homepage: www.elsevier.com/locate/mseb

Microstructure and soft magnetic properties of $(Fe_{0.9}Co_{0.1})_{73.5}Si_{13.5}B_{9-x}Nb_3Cu_1Ge_x$ nanocrystalline alloys

Li Zhang, Zhi Wang*, Yu-rong Jia

School of Science, Tianjin University, Tianjin 300072, China

ARTICLE INFO

Keywords:
Amorphous materials
Magnetic materials
Nanocrystalline materials
Soft magnetic properties
Exchange coupling

ABSTRACT

The nanocrystalline $(Fe_{0.9}Co_{0.1})_{73.5}Si_{13.5}B_{9-x}Nb_3Cu_1Ge_x$ alloys were obtained by partial devitrification of their amorphous precursors. The influence of partial substitution of B by Ge on the microstrucural evolution of these alloys was studied by means of X-ray diffraction (*XRD*) and differential scanning calorimeter (*DSC*). The temperature dependence of initial permeability (μ_i-T curves) for $(Fe_{0.9}Co_{0.1})_{73.5}Si_{13.5}B_6Nb_3Cu_1Ge_3$ alloys heating–cooling cycled at 450–650 °C was mainly measured. It was found that the Ge doping into $(Fe_{0.9}Co_{0.1})_{73.5}Si_{13.5}B_9Nb_3Cu_1$ alloy can reduce the onset primary crystallization temperature (T_{x1}), enlarge the interval temperature (ΔT_x) from 129 °C to 180 °C and improve the high temperature soft magnetic properties, especially for $(Fe_{0.9}Co_{0.1})_{73.5}Si_{13.5}B_6Nb_3Cu_1Ge_3$ alloy. After annealed at 450–650 °C for the alloy with $x = 3$, the optimum high temperature magnetic softness was observed in 600 °C-annealed sample, the μ_i above 1000 at 10 kHz can be kept up to 550 °C, which is due to the higher crystallization phase volume fraction and the thinner amorphous layer thickness and an enhancement of the exchange stiffness in the intergranular region.

1. Introduction

Fe-based nanocrystalline alloy with the typical composition of $Fe_{73.5}Si_{13.5}B_9Nb_3Cu_1$ shows outstanding soft magnetic properties [1]. The ultra-soft magnetic properties is due to the particular two-phase structure consisting of α-Fe(Si) nanocrystallites embedded in amorphous matrix [2]. However, the Curie temperature (T_c^{am}) of the residual amorphous phase is relatively low, and the nanocrystals become uncoupled when the temperature is above the T_c^{am}. With the aim of increasing the T_c^{am}, Co was added to partially substitute for Fe in Finemet, then improved the magnetic properties at high temperature [3–5]. Unfortunately, superfluous Co causes the deterioration of magnetic softness because of the larger saturation magnetostriction [6] and the larger magneto-crystalline anisotropy [7,8]. Therefore fewer Co is chosen to dop into Finemet, which is expected to improve both room- and high-temperature magnetic softness.

The crystallization mechanism of the two-phase nanocrystalline alloy consists of four stages: the first stage is the obtainment of amorphous alloy from the ingot by the single-roller melt spinning method; during the second stage, clustering of Cu preferential grow and the density can reach $10^{24}/m^2$. Next stage, heterogeneous nucleation of α-Fe phase around the Cu clusters. Optimum stage, the α-Fe(Si) nanocrystalline grains are obtained and form into a soft magnetic dual-phase alloy with the amorphous matrix, as core/shell-like nanocomposite magnets [9].

It was also reported that when Ge is added to the Finemet alloy for partially replacing B, it shows very low values of coercivity and improved soft magnetic properties of the alloys [10]. Furthermore, the doping Ge into Fe-based nanocrystalline alloys could enhance the Curie temperature of amorphous phase by about 60 °C [11]. Hence $(Fe_{0.9}Co_{0.1})_{73.5}Si_{13.5}B_{9-x}Nb_3Cu_1Ge_x$ alloys are designed for further improving magnetic softness both in room and elevated temperatures.

2. Experimental procedure

Amorphous ribbons, 20 μm thick and 1 mm wide, were obtained from the ingot by the single-roller melt spinning method. The melt-spun ribbons were wound into cores with an outer diameter of about 18 mm and inter diameter of 16.3 mm. The samples were submitted to isothermal treatment for 0.5 h under vacuum atmosphere in order to obtain the characteristic nanocrystalline structure. The crystallization temperature of as-spun ribbons were measured by a different scanning calorimeter (DSC) at a heating rate of 40 °C/min. The microstructure of the amorphous and annealed ribbons was examined by X-ray diffraction (XRD) using D/max-2500/PC with Cu-K_α radiation ($\lambda = 1.54056$ Å). The initial permeability was measured by using HP4294A impedance analyzer at $H = 0.4$ A/m and $f = 10$ kHz under Ar atmosphere protection in the temperature range of 30–700 °C.

* Corresponding author.
E-mail address: zhiwang@tju.edu.cn (Z. Wang).

https://doi.org/10.1016/j.mseb.2017.12.028
Received 10 August 2017; Received in revised form 6 December 2017; Accepted 27 December 2017

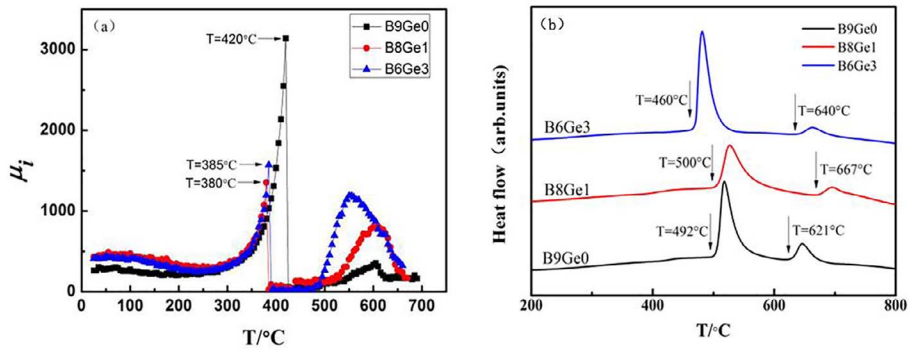

Fig. 1. μ_i -T curves (a) and DSC (b) curves of as-quenched $(Fe_{0.9}Co_{0.1})_{73.5}Si_{13.5}B_{9-x}Nb_3Cu_1Ge_x$ (x = 0, 1, 3) alloys.

Table 1
Values of the onset primary and secondary crystallization temperatures (T_{x1} and T_{x2}), the interval temperature ΔT_x ($\Delta T_x = T_{x2} - T_{x1}$), as well as the Curie temperature (T_c^{am}) for as-quenched $(Fe_{0.9}Co_{0.1})_{73.5}Si_{13.5}B_{9-x}Nb_3Cu_1Ge_x$ (x = 0, 1, 3) alloys.

Composition	T_{x1} °C	T_{x2} °C	ΔT_x	T_c^{am} °C
$(Fe_{0.9}Co_{0.1})_{73.5}Si_{13.5}B_9Nb_3Cu_1$	492	621	129	420
$(Fe_{0.9}Co_{0.1})_{73.5}Si_{13.5}B_8Nb_3Cu_1Ge_1$	500	667	167	380
$(Fe_{0.9}Co_{0.1})_{73.5}Si_{13.5}B_6Nb_3Cu_1Ge_3$	460	640	180	385

3. Results and discussion

The temperature dependence of initial permeability (μ_i-T) was measured for the Curie temperature as well as high-temperature magnetic response of as-quenched $(Fe_{0.9}Co_{0.1})_{73.5}Si_{13.5}B_{9-x}Nb_3Cu_1Ge_x$ (x = 0, 1, 3) alloys is shown in Fig. 1(a). On all curves, a characteristic sharp Hopkinson peak was observed at T_c^{am}, which is due to the more quickly decreasing of magnetic anisotropy than that of the saturation magnetization. It can be seen that the T_c^{am} of $(Fe_{0.9}Co_{0.1})_{73.5}Si_{13.5}B_{9-x}Nb_3Cu_1Ge_x$ (x = 0, 1, 3) alloys are 420 °C (x = 0), 380 °C (x = 1) and 385 °C (x = 3). When temperature is just above T_c^{am}, the μ_i drops to zero, which is attributed to the transition from ferromagnetic to paramagnetic state of the amorphous alloy. Above 500 °C, the μ_i rise up, reflecting a successive precipitation of strongly coupled ferromagnetic crystalline phase with magnetic softness from paramagnetic amorphous matrix. Then the μ_i shows a succedent decrease which may be associated with the formation of the boride phase or ferro-paramagnetic transition of crystalline phase. The addition of Ge into $(Fe_{0.9}Co_{0.1})_{73.5}Si_{13.5}B_9Nb_3Cu_1$ alloy decreases the T_c^{am} which is maybe that Ge consumes Fe in amorphous phase and diminishes the stronger exchange interaction between Fe and Co atoms largely as Ni [12].

Fig. 1(b) shows the crystallization processes of the as-quenched $(Fe_{0.9}Co_{0.1})_{73.5}Si_{13.5}B_{9-x}Nb_3Cu_1Ge_x$ (x = 0, 1, 3) alloys determined by *DSC*. Each curve shows two separated exothermic peaks corresponding to the two-stage crystallization process. The first crystallization stage is correlated to the precipitation of crystallized soft magnetic phases α-Fe (Si,Ge) and Fe_3(Si,Ge) at lower temperature. The second one is associated to the formation of hard magnetic phase. The onset primary crystallization temperature (T_{x1}), second crystallization temperature (T_{x2}) and crystallized interval temperature (ΔT_x) are shown in Table 1. It can be seen that the addition of Ge decreases the T_{x1} (x = 3) and increases T_{x2} (x = 2 and 3), respectively. The alloy with x = 3 exhibited the largest ΔT_x about 180 °C, which guarantees a broader temperature range for the precipitation of the single crystalline phase. The stabilization mechanism is due to preferential partitioning of Ge in the residual amorphous phase [13] and the substitution of Ge for B increase the temperature of boride precipitation in a continuous heating process [14].

The results of the X-ray diffraction (*XRD*) experiment of as-quenched and annealed $(Fe_{0.9}Co_{0.1})_{73.5}Si_{13.5}B_6Nb_3Cu_1Ge_3$ samples are shown in Fig. 2(a). The diffraction pattern of the as-quenched ribbon exhibits one broad scattering peak, indicating that the quenched ribbon is fully amorphous. However, the ribbons annealed at 500–650 °C show the characteristic diffraction peaks corresponding to crystalline precipitation. All the annealed samples show the characteristic (1 1 0), (2 0 0) and (2 1 1) diffraction peaks for bcc α-FeCo(Si,Ge) phase and the ordered characteristic (2 2 0) diffraction peak for Fe_3(Si,Ge) phase. For the 650 °C annealed sample, the diffraction peak of Fe_2B hard magnetic phase is detected.

The volume fraction of the crystalline phase (V_{cry}) is obtained from the integral intensity of diffraction peak of (1 1 0). The equation is as follows [15]:

$$V_{cry} = I_{cry}/(I_{cry} + KI_{am}) \quad (1)$$

where I_{cry} and I_{am} are the diffraction intensities of the crystalline and

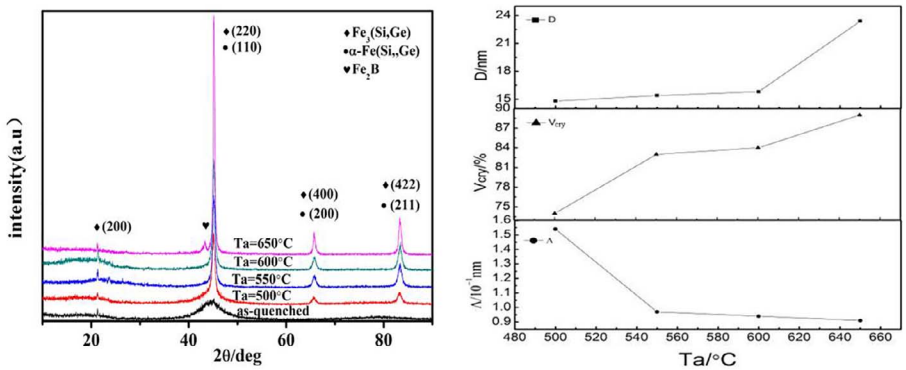

Fig. 2. XRD patterns (a) of as-quenched and annealed $(Fe_{0.9}Co_{0.1})_{73.5}Si_{13.5}B_6Nb_3Cu_1Ge_3$ samples and crystalline volume fraction (V_{cry}), average grain size (D), and thickness of intergranular amorphous layer (Λ) (b) for annealed $(Fe_{0.9}Co_{0.1})_{73.5}Si_{13.5}B_6Nb_3Cu_1Ge_3$ samples at 500–650 °C.